Thesis for the degree of Licentiate of philosophy
in
Machine and Vehicle Systems

Target-driven road vehicle suspension design
licentiate thesis

YANSONG HUANG

Department of Mechanics and Maritime Sciences
CHALMERS UNIVERSITY OF TECHNOLOGY
Göteborg, Sweden 2022

Target-driven road vehicle suspension design
LICENTIATE THESIS

YANSONG HUANG

Licentiate thesis at Chalmers University of Technology
Technical report No. 2022:14

Department of Mechanics and Maritime Sciences
Chalmers University of Technology
SE–412 96 Göteborg
Sweden
Telephone: +46 (0)31–772 1000

Cover:
Suspension hardpoint setup with different targets from Paper A.

Chalmers Reproservice
Göteborg, Sweden 2022

Target-driven road vehicle suspension design

LICENTIATE THESIS

Yansong Huang
Department of Mechanics and Maritime Sciences
Chalmers University of Technology

Abstract

This thesis is focused on suspension hardpoint and bushing compliance design with new reverse engineering methods that are based on kinematics and compliance constraints. The kinematic reverse design method is implemented into a conceptual front axle development. The results show that, using this method, the design lead time is reduced by half. It is concluded that the design of the suspension architecture can be more efficient and precise by automatic suspension design algorithms.

The wheel suspension is one of the most architecture-heavy systems in a car and much of the car's overall motion characteristics and limitations are determined by it. Among other things, electrification, and fierce global competition place ever higher demands on faster and more efficient development of new vehicle concepts, even within a classic area such as mechanical wheel suspension design. The wheel suspension system has many design parameters and prerequisites that have very complex relations. Traditionally the development process has been dependent on very skilled engineering teams. A clear bottleneck in the development of a new wheel suspension today is how to balance the complex performance requirements and which today require time-consuming calculations to evaluate for each iteration of the design. One solution to the above problem can be to look over the total development process, from target setting to verification, via re-design or optimization loops.

Keywords: Kinematics, compliance, suspension, reverse design, target

Acknowledgments

I would like to express my sincere gratitude to my industrial supervisor Tobias Brandin for initiating the project and providing invaluable guidance throughout the research. His expert experience brings the project on a higher level. It was my honor to work and study under his guidance. I am also extremely grateful to suspension architecture team at Volvo Cars. I would like to thank my manager Jenny Berglund for the administrative support and my colleague Naik Akshay, Daniel Molin for all the help.

In my division at Chalmers University of Technology, I would like to express my special thanks to my academic supervisor Prof. Bengt Jacobson and Prof. Krister Wolff for supervising on a higher level and asking the fundamental questions. I am thankful to Sonja for taking care of the administrative thing. I am also thankful to my examiner Prof. Mattias Wahde for his help. My supervision group from Research Institute for Automotive Engineering and Powertrain Systems Stuttgart (FKFS) has provided a great learning opportunity and has established an excellent cooperation. Special thanks to Dr. Jens Neubeck from FKFS for his supervision and administrative work. I would also like to express my gratitude to my colleague Johannes Köpler for all technical and non-technical discussions we have had.

This thesis would not have been possible without funding partner: VINNOVA of the Fordonsstrategisk forskning och innovation (FFI).

Last but not least, thanks for my family for your encouragement. Thanks for countless support and love.

Yansong Huang
Göteborg, November 2022

Thesis

This thesis is based on the following appended papers:

Paper A
Huang, Y., Tobias, B., and Jacobson, B., Linear and nonlinear kinematic design of multilink suspension. **Manuscript accepted** in SAE International Journal of Passenger Vehicle Systems on August. 26, 2022.

Paper B
Huang, Y., Köpler, J., Wagner, A., Neubeck, J., and Jacobson, B., "Optimized Rear-Axle Concept for Battery Electric Vehicles," Proceedings of the *6TH SHANGHAI-STUTTGART-SYMPOSIUM AUTOMOTIVE AND POWERTRAIN TECHNOLOGY*. December 1-2, 2022, Shanghai

Paper C
Naik, A., Tobias, B., Huang, Y., A., and Jacobson, B., "Target driven bushing design for wheel suspension concept development," Submitted to *WCX SAE World Congress Experience*. April 18-20, 2023, DETROIT

and patent applications:

i
Daniel Molin, Mikael Sellergren, Tobias Brandin, and Yansong Huang, "Stable rear wheel steering geometry for Integral rear suspension," Chinese patent application no. CN114633594A, 2022.

Nomenclatures

$\mathbf{V}$	[mm/s]	Translational velocity at wheel center O for jounce motion
ω	[rad/s]	Rotational velocity at wheel center O for jounce motion
$\mathbf{a}$	[mm/s^2]	Acceleration at wheel center O for jounce motion
α	[rad/s^2]	Angular acceleration at wheel center O for jounce motion
$\mathbf{V}_p$	[mm/s]	Translational velocity at Contact patch P for jounce motion
$\mathbf{a}_p$	[mm/s^2]	Acceleration at contact patch P for jounce motion
$\mathbf{V}^{'}$	[mm/s]	Translational velocity at wheel center O for steering motion
$\omega^{'}$	[rad/s]	Rotational velocity at wheel center O for steering motion
$\mathbf{a}^{'}$	[mm/s^2]	Acceleration at wheel center O for steering motion
$\alpha^{'}$	[rad/s^2]	Angular acceleration at wheel center O for steering motion
$\mathbf{V}_p^{'}$	[mm/s]	Translational velocity at Contact patch P for steering motion
$\mathbf{a}_p^{'}$	[mm/s^2]	Acceleration at contact patch P for steering motion
K_A	[%]	Ackermann percentage
l	[mm]	Wheel base
δ	[deg]	Toe angle
γ	[deg]	camber angle
R_s	[mm]	Rack travel
$\mathbf{F}_O$	[KN]	Force at wheel center O
$\mathbf{F}_p$	[KN]	Force at contact point P
$\mathbf{M}$	[KN $\cdot$ mm]	Torque at wheel
$\hat{\mathbf{V}}, \hat{\omega}$		Geometric vectors

Table of Contents

Chapter 1

Introduction

The wheel suspension design faces many challenges and need requirements from many attributes like ride comfort, handling and steering (kinematics and compliance), see Figure 1.1 as well as packaging, styling, durability, noise and vibration (NVH) requirements. The design must achieve all these aspects to have the expected overall behaviors. Most of the kinematic behavior is nonlinear with complex kinematic relationships between parameters and key performance indicators (KPI) evaluating the wheel motion. Furthermore, compliance further increase the system nonlinearity and thereby makes the tuning difficult. Packaging is also a factor that constrains the parameter selection. The complexity of multiple requirements, within a vehicle and within a platform or architecture, is another important factor compounding the design challenges faced by the concept engineers. Since multilink suspensions are typically employed to accomplish the best overall performance, it is important to understand this system better by using new methods to solve complex nonlinear problems in shorter time.

Current methods to verify requirements on wheel suspension design typically rely on axle level simulations. These simulations are done by multi-body system software (MBS). Suspension systems are parameterized by springs, dampers, joint and bushing locations (hardpoints) and compliance, see Figure 1.1. Improvements are then found by testing different combination of hardpoints and bushing parameters. In many cases, this process is manual trial-and-error, and it is thus normally slow. In some cases, optimization is used, but optimization is typically difficult to set up and is still rather time-consuming since many simulations are required. It also takes some time and human guidance to set up the optimizations. The workflow combines different software tools. Thus, information sharing between different tools consume a lot of time. Methods for calculating the kinematics of suspension have been developed [1, 2, 3]. With the help of visualization methods introduced in [4, 5, 6], engineers can calculate and analyze the kinematics performance directly from given hardpoints. The compliance design mainly concerns

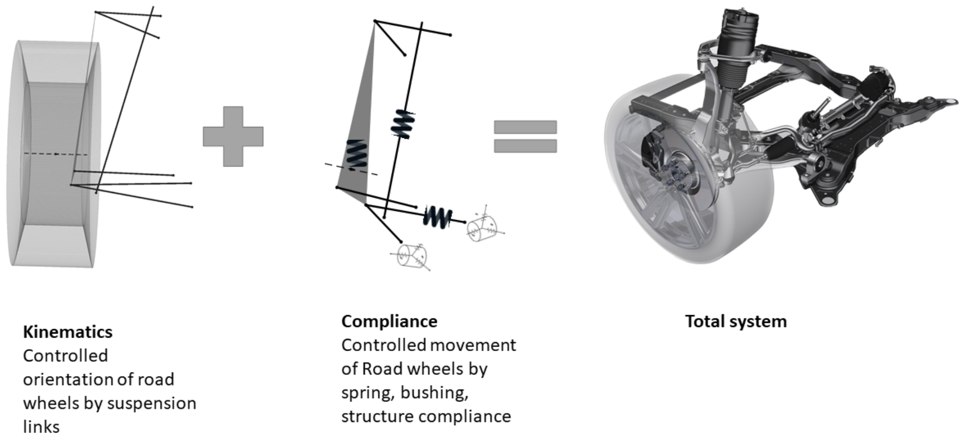

Figure 1.1: Wheel suspension kinematics and compliance [7].

the bushing elasticity. Methods to simulate the compliance behaviors have been developed [8, 9, 10]. The modelling methods and simulation methods convert the hardpoints setups and bushing specifications to behaviors reports such as kinematic and compliance reports. The axle level targets in this thesis need to meet the requirements from attribute leaders. The process is time-consuming while the targets are difficult to meet considering all the attributes, and the fact that the targets are constantly changing during the vehicle development project. The axle design iterating with targets are critical parts within complete vehicle development processes. Section 1.1 introduces how the wheel suspension development interacts with the complete vehicle development process, and a method to reduce the manual iterations.

The project consider here will result in knowledge, methods, and tools for semi-automatic translation of wheel suspension axle requirements into a suggested hardpoints and bushing setup. The tool shall be designed for suspension engineers, which will enable agile working method with target-based design and quick adaption to changing requirements. Concept selection will be much quicker, and engineers are anticipated to develop a much better understanding of the system. More time is thereby expected to be available to improve cost, quality, durability, and weight. One of the tasks in this project is to quantification of how much quicker and which quality gains have been achieved. Typically, the aim to measure the time and quality from updated requirements to a new design proposal. A tool that involves all concept suspension development process is required, and it should provide a user-friendly interface.

1.1 Background

A typical development process for passenger car follows a standard flow from project definition until start of the production. A well-known development process 'V model' is used to break down the whole process into concept phase and validation phase. Figure 1.2 shows the milestones during the V process. The flow also shows three groups including complete vehicle, subsystems and components. Lots of simulations are used to define the targets for each group and verifications. To achieve certain goal from the complete vehicle perspective, a method called targets cascading is used to break the targets from top floor to bottom floor. The break-down process needs to ensure a qualified tuning scopes and correlate the targets between different subsystems and components. After the concept phase, the validation phase ensures the targets are meet from each level. The simulations and prototype cars are used to evaluate both subjective and objective targets. However, the V process needs to iterate between the concept phase and the validation phase since a huge mount of system balancing and comprising works are part of the process. Therefore, the development lead time is usually a couple of years depend on the customer requirements.

A typical development process of a passenger car follows a flow from project definition to start of the production. A development process can use the 'V model' to explain different levels and the mechanisms of requirement setting and requirement verifying. Figure 1.2 shows both the milestones of the process and the V model. A vehicle is a very complex product, in terms of many subsystems and in terms of many requirements to fulfill. A huge amount of iterations is needed in the development to handle all necessary compromises. To cut the development time, one arranges the work in levels, here: complete vehicle, subsystems and components. Still, the development time is usually a couple of years.

To work in levels, the requirements on the complete vehicle performance has to be cascaded (broken down) to each lower level. To gain time and preciseness, nowadays it is customary to cascade more and more on simulations. For example, at the complete vehicle level, one makes simulations to find out which requirements to send to each subsystem (e.g.front axle) as well as simulations that checks if the resulting designs of the subsystems give good enough complete vehicle performance. Similarly, at the subsystem level, one makes simulations to find out which requirements to send to each component (link and bushing) as well as simulations that checks if the resulting design gives good enough axle performance. The simulations on different levels can, in some design loops, be replaced with real world tests in rigs, test cars, or driving simulators. Test cars and driving simulators have the advantage that subjective requirements can be assessed. In wheel suspension development process, the targets usually come from the complete vehicle level. The targets are formulated in kinematics and

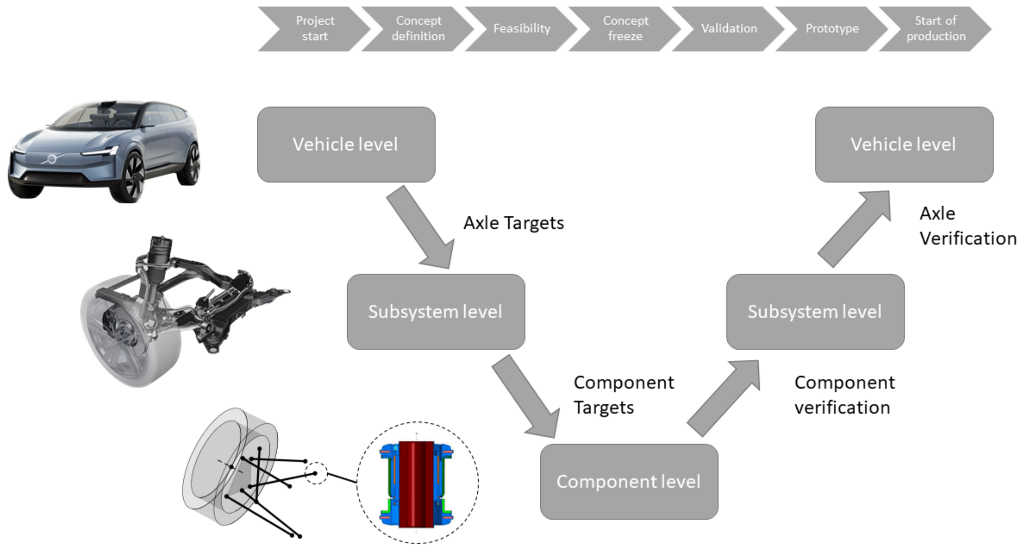

Figure 1.2: V development process [7, 11, 12].

compliance performances of the axle. Hence, the design decisions of each axle include hardpoint coordinates and bushing specifications. Also, springs, anti-roll bar and damper are design decisions of each axle, but those are not in focus for this thesis. The hardpoint design influence attributes, for example, packaging, handling, compliance, durability, ride comfort, NVH and styling. Therefore, the decision of hardpoint coordinates as bottom level in the V process must go through several iterations to satisfy the targets from all the attributes. The traditional knowledge-based trial-and-error method is way too slow especially considering the high requirements from electric vehicle and increasing active systems. The concept compliance design further complicates the traditional iterate process. Due to the reasons mentioned above, a method for generating the hardpoint coordinates and bushing specifications automatically is proposed by the author.

1.2 Research question

The research question is essentially to reverse the simulation process from components design to resulting performance measures for an axle. More specifically, the new idea is to generate the hardpoints and bushing specification from given targets automatically. The originality of this project is believed to be the reverse method which represents the human experience. The focus is on reversing the simulations, to go directly from a set of targets to a limited set of hardpoints and bushing setups that fulfil the requirements. From the kinematic perspective, the method provides certain hardpoints design guidelines with specific linear and nonlinear targets. The model allows for the introduction of more targets and hence of reducing the design degree of freedom even further. From compliance points of view, the research question is to set up the bushing stiffness specification according to compliance targets. Addition to engineering side, the project aim to contribute the competence to effectively develop new vehicle concepts of which the wheel suspension are integral parts. These questions are initialized below:

- How can suspension design be supported by reverse methods to improve the overall vehicle development process? How to shorten the design lead-time by using targets oriented reverse design methods?
- Which modelling, virtual methods (simulation, computation) and requirement settings are needed to connect between vehicle and suspension design?

1.3 Contribution

The contribution of this work is that it provides an automatic method which sets the hardpoint and bushing specification from given kinematics and compliance targets. The method is verified through a case study about a new suspension geometries for electric vehicle. The thesis provides opportunities for better system understanding and efficiency of large-scale system optimization in product development and product architecture development. The method also gives decision support and risk assessment in vehicle development through proper insight into the coupling of product requirements and design parameters in the concept phase. The contributions and findings are summarized as following:

I. Traditional suspension design methods based on trial-and-error is not efficient. Suspension engineers must meet packaging constraints by relying on trial-and-error iterative simulations to gradually refine the kinematic performance. Simulating suspension behaviors is also time-consuming. Therefore, a method that reduces the kinematic design lead time has been proposed. The method presented primarily addresses the kinematic design problem by reversing the traditional design procedure. The algorithm which starts from target identification provides design guidelines, including linkage orientation, length and position. The method includes calculations in two steps. The first step is to obtain the velocity constraints and to use first-order linear targets to calculate general motions. Then the hardpoints design guideline for the first order targets control is provided from the algorithm to designers by indicating the linkage directions. The second step uses higher order targets (acceleration and jerk constraints), which can be obtained by partial differentiation from velocity and acceleration constraints. The exact position of the linkage can then be calculated with these higher order targets. The results show that the general motion, which includes velocity, acceleration, and jerk, is precisely controlled by this method. The result also shows that the complete design can be approached simultaneously from a feasible packaging solution and required kinematic setup, and eventually transfers into a solution that satisfies both packaging and kinematic requirements. The reverse method helps design engineers search the feasible packaging solutions more efficiently in the early design stages. Furthermore, compared with previous optimization-based methods, the new method here always provides unique solutions, which means that the targets and the hardpopints are uniquely correlated. Therefore, engineers who work with CAE and CAD parts can always build clear connections to each other by understanding the influence from both the performance and the packaging side. (Paper A)

II. To meet the complex requirements, the design of a new suspension concept is usually time-consuming. The suspensions' kinematics and packaging need to be considered simultaneously, since they influence each other. A method or process for how to design for both kinematic requirements and packaging requirements is developed and demonstrated. The goal of this work is to invent a new suspension system for a battery electric vehicle with a maximized battery volume. The underlying algorithms are used to handle the kinematics and packaging automatically. Critical improvements during the development is demonstrated within show cases and subsequently discussed. The tuning process starts from a suspension used in a traditional combustion vehicle, and eventually is adapted to the needs of a battery electric vehicle. The automatic kinematic tuning method is used to maintain the performance targets for each iteration, while the automatic packaging tool is used to search for a feasible packaging solution. The show cases confirm the efficiency of both kinematics and packaging methods. Eventually, the new suspension layout provides extra 130mm for battery. The results prove the possibility to synchronize the kinematics tuning and packaging processes. Thanks to the automatic methods, the design leading time has been dramatically reduced. (Paper B)

III. The traditional bushing tuning method involves an optimization process in Adams Car or any other multi-body simulation software. Although it provides reliable results, it is a time-consuming process to build models for the complete kinematics and compliance analysis. Therefore, a method to reduce the bushing tuning time has been proposed. It applies the reverse algorithms to calculate the bushing stiffness values along the link directly from the compliance targets for a given hardpoint setup, and provides guidelines for the proper bushing design in the early phase of the concept development. The method includes the calculation of motion ratios and force distribution as a function of the hardpoint setup. So, regardless of the compliance targets and bushing stiffness values, these ratios remain constant as long as hardpoints are unchanged. Further, these ratios are used to study the possible effect on the wheel orientation if bushings are used as a bushing sensitivity study. Then the exact stiffness of the bushings at the inner hardpoints is calculated by specifying the compliance targets. (Paper C)

1.4 Thesis outline

The presented contributions are appended with papers. The thesis will further discuss the methods for nonlinear suspension steering kinematics design at section 3.1, and section 3.2 introduces a method design the conceptual bushing compliance. Section 3.3 combines the two methods above and integrates them into the overall suspension development process. A front suspension is used as demonstration example in section 3.3. Chapter 4 discusses the method used for reverse design. Chapter 5 summarizes the work with a discussion, conclusion and future work.

Chapter 2

Review of appended papers

The work has been divided in two parts. They are the kinematic reverse design method and the compliance reverse design method. An algorithm presented in Paper A is focused on automatic hardpoints design method for a rear axle. A proposal using Jacobian differentiation of the position constraints is used to generate hardpoints with given targets. A new process to reverse-engineer a geometry set based on kinematic performance constraints is proposed. The method also applies to a front axle. Section 3.1 discusses the new targets for the front axle. Since a larger steering angle is required from the front axle, an algorithm that helps the design of Ackermann percentage is presented at Section 3.1.2. An important concept to achieve the automatic hardpoint tuning method is the control points which discussed in Paper A in section 4.2.1. Therefore, the inputs to the automatic hardpoint design method are categorized as the targets and the control points. Paper B illustrates how the suspension packaging problem solved by changing the control points. It shows an efficient way of working to combine the automatic packaging method and the automatic hardpoint setting method. Paper B uses new developed method to investigate a concept design for electric vehicle. The goal is to design a new rear suspension concept to maximize the battery space. The work involves lots of design iterations for both kinematics and packaging. The method is developed to automatically set up the hardpoint according to targets, which has been approved as an efficient way to reduce the manual iterations. The control point concept also shows a great potential to reduce the packaging iterations together with the automatic packaging method. The kinematics method sets a good baseline for a concept suspension. However, to deliver a sufficient concept model, suspension compliance is also important to be designed efficiently. Paper C shows a method for suspension compliance design. The goal is similar to the kinematic design method. The bushing stiffnesses are calculated from given compliance targets. The method uses the superposition principle with linearized suspension model. The algorithm has three steps namely calculation of motion ratios, force distributions and the reverse method using linear algebra. The results from Paper C shows a good match between the input targets and the simulated results. Section 3.3 shows an idea combining the kinematics method and the compliance method as a workflow for concept suspension design. An example is used to demonstrate the methods. In the end, the results show a pipeline that well connects the methods mentioned in different parts. It can help the concept suspension design in an efficient way.

Chapter 3

Method and results

3.1 Suspension kinematic design for front axle

The kinematic design of a steerable front suspension is time-consuming. The front suspension of a passenger car should ensure a high level driving dynamic and smooth steering feeling. Therefore, the requirements applied on characteristic curves are demanded. The characteristic curves included steering and jounce motions need to be tuned carefully to secure the targeted kinematic behaviors. The targets that reflect the suspension steering performance have been studied in a large scope [17, 19, 18]. Some targets can be measured from geometrical setup [20, 21], and some targets can be defined through mathematic expressions, for example, Paper A. Optimizations are employed to solve the kinematic problem in different formats [16, 22, 23]. The author has the ambition to fully automatize the hardpoint development process by pre-select the targets. The objective of this chapter is to provide a method that automatically tune hardpoints with given performance targets, and it also considers the packaging constraints. The method consists of several algorithms that take care of different optimization routines. First, the method optimizes the linearized constraint matrices by means of given performance targets as input, and then the second optimization routine takes care of Ackermann behavior on top of the first optimization. In the end, a hardpoints configuration is proposed by the automatic method. It was found that the method can handle the complex design task by considering all the targets simultaneously, and the shorted design lead time shows the capability of the proposed procedure.

3.1.1 Nonlinear behaviors of steering motion

Paper A has identified a scope of targets as they are shown in table 3.1 and 3.2. These tables reflect the targeted performance of a steerable rear axle. For a steerable front axle, the targets need to be modified to fulfil the evaluation criteria.

The pre-selected targets for the font axle are shown in next section called target identification.

1st Bump Steer	2nd Bump Steer	3rd Bump Steer
1st Bump Camber	2nd Bump Camber	3rd Bump Camber
1st (Kinematic) Anti-squat	2nd Anti-squat	3rd Anti-squat
1st (Kinematic) Anti-lift	2nd Anti-lift	3rd Anti-lift
1st Roll center height (RCH)	2nd RCH	3rd RCH

Table 3.1: Jounce targets for steerable rear axle.

Hub Trail
Scrub Radius
Kingpin offset
Caster trail
Wheel load lever arm (WLLA)

Table 3.2: Steering targets for steerable rear axle.

Target identification

For a steerable front axle, the focus should be on the steering motion, which is why it cannot only change numerical values of the targets from a rear axle. It is motivated to change the targets from the ones in tables 3.1 and 3.2 to the ones in tables 3.3 and 3.4. Note that the number of targets is kept the same. However, the second order hub trail and kingpin offset are replaced by the change of the caster angle and the kingpin angle. The change of these two angles implicitly controls the camber change versus steering angle. The requirement on the second order kingpin-offset is usually not critical, and second order hub trail is more related to drive shaft design.

1st Bump Steer	2nd Bump Steer
1st Bump Camber	2nd Bump Camber
1st (Kinematic) Anti-squat	2nd Anti-squat
1st (Kinematic) Anti-lift	2nd Anti-lift
1st Roll center height (RCH)	2nd RCH

Table 3.3: Selected jounce targets for front axle.

Hub Trail	2nd kingpin angle
Scrub Radius	2nd Scrub Radius
Kingpin offset	2nd Caster angle
Caster trail	2nd Caster trail
Wheel load lever arm (WLLA)	2nd WLLA

Table 3.4: Steering targets for front axle.

Most of the targets that are shown in tables 3.3 and 3.4 are identified in Paper A. The rest of the targets are identified here. To define the measure of the target, the general motion at wheel center assume to be known. The method to derive the general motion is described in Paper A. The general motion $\mathbf{V}'$, ω', $\mathbf{a}'$, α' at wheel center and $\mathbf{V}_p'$, $\mathbf{a}_p'$ at contact point can be calculated using same method.

$$\text{2}^{\text{nd}} \text{ kingpin angle} = \frac{1}{1+\frac{\omega_x'^2}{\omega_z'^2}} \cdot \frac{\alpha_x'}{\omega_z'^2} \tag{3.1}$$

$$\text{2}^{\text{nd}} \text{ Scrub Radius} = \frac{(a_{px}'cos(\delta) - a_{py}'sin(\delta))\omega_\delta' - \alpha_\delta'(V_{px}'cos(\delta) - V_{py}'sin(\delta))}{\omega_\delta'^2\omega_z'} \tag{3.2}$$

$$\text{2}^{\text{nd}} \text{ caster angle} = \frac{1}{1+\frac{\omega_y'^2}{\omega_z'^2}} \cdot \frac{\alpha_y'}{\omega_z'^2} \tag{3.3}$$

$$\text{2}^{\text{nd}} \text{ Caster trail} = \frac{(-a_{px}'sin(\delta) - a_{py}'cos(\delta))\omega_\delta' - \alpha_\delta'(-V_{px}'sin(\delta) - V_{py}'cos(\delta))}{\omega_\delta'^2\omega_z'} \tag{3.4}$$

$$\text{2}^{\text{nd}} \text{ WLLA} = \frac{a_{pz}'\omega_\delta' - \alpha_\delta' V_z'}{\omega_\delta'^2\omega_z'} \tag{3.5}$$

where,

$$\omega_\delta' = -\omega_x'tan(\gamma)sin(\delta) - \omega_y'tan(\gamma)cos(\delta) + \omega_z'$$
$$\alpha_\delta' = -\alpha_x'tan(\gamma)sin(\delta) - \alpha_y'tan(\gamma)cos(\delta) + \alpha_z'$$

Method to reverse the analysis

From Section 3.1.1, the general motions $\mathbf{V}$, $\omega, \mathbf{a}$, α for jounce motion and $\mathbf{V}'$, $\omega', \mathbf{a}'$, α' for steer motion at wheel center can be calculated from targets which are shown in tables 3.3 and 3.4. The control points explained in Paper A are used to interact with the packaging conflicts. Furthermore, to fully automatize

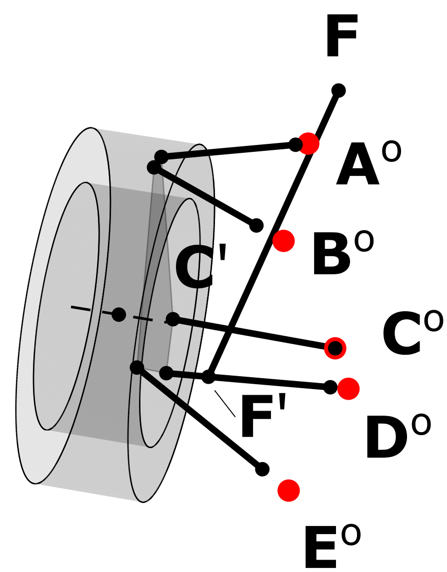

Figure 3.1: Pre-set parameters for front axle.

the program, some other parameters are given as inputs. The additional inputs are chosen as F_z, F'_y, C'_x and C'_y.

The optimization process follows the similar method as stated in Paper A. The inner and outer hardpoints can be calculated from the method.

3.1.2 Design algorithms considering Ackermann angle

The Ackermann percentage K_A measures the turning property with large steering angle. Usually at least 20 to 30 percent are required from a passage car to ensure a smooth turning without tire-wear problem. To ensure a reasonable Ackermann percentage, the suspension needs to be carefully designed. The maximum steering angle left δ_L and right δ_R need to be controlled in such a way that achieve required Ackermann percentage. Figure 3.2 shows the parameters to identify the Ackermann percentage.

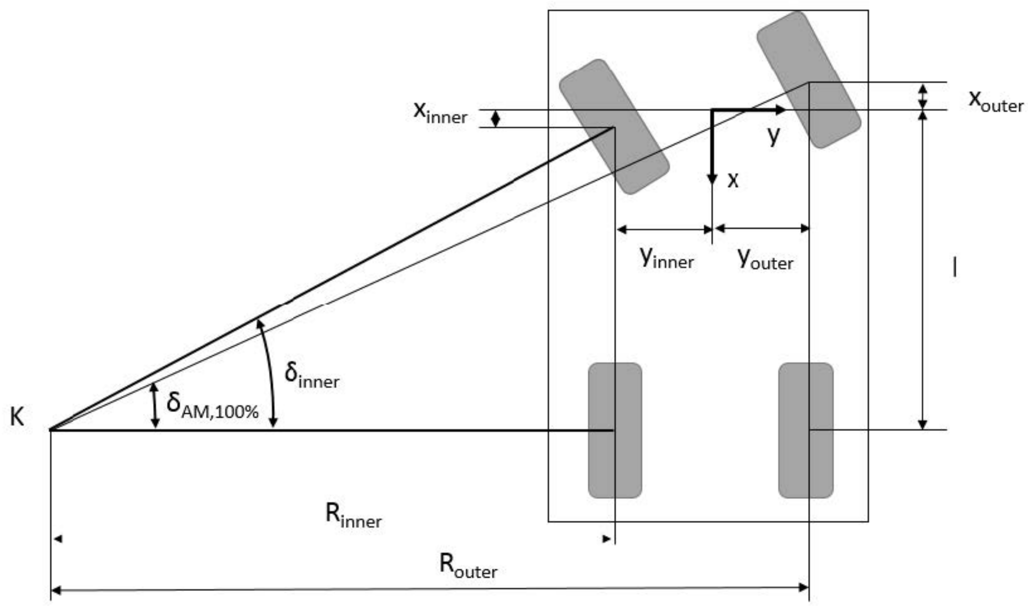

Figure 3.2: Configuration of Ackermann angle.

With maximum rack travel, the Ackermann percentage measures the difference between the Ackermann angle 100% and the real angle between δ_L and δ_R. The Ackermann angle 100% is defined respect to inner angle (left) at this case. $\delta_{AM,100\%}$ can be expressed through triangular relationship,

$$\delta_{AM,100\%} = \frac{l - x_{outer}}{R_{inner} - y_{inner} + y_{outer}} \tag{3.6}$$

with the expression of δ_{inner},

$$\delta_{inner} = \frac{l + x_{inner}}{R_{inner}} \tag{3.7}$$

then,

$$\delta_{AM,100\%} = \frac{l - x_{outer}}{\frac{l+x_{inner}}{tan(\delta_{inner})} - y_{inner} + y_{outer}} \tag{3.8}$$

Therefore, the expression of Ackermann percentage K_A will be,

$$K_A = \frac{\delta_{inner} - \delta_{outer}}{\delta_{inner} - \delta_{AM,100\%}} \cdot 100\% \tag{3.9}$$

For left turning is shown in figure 3.2, δ_{inner} means δ_L, and δ_{outer} means δ_R. The maximum left steering angle δ_L is considered as the toe change because of the

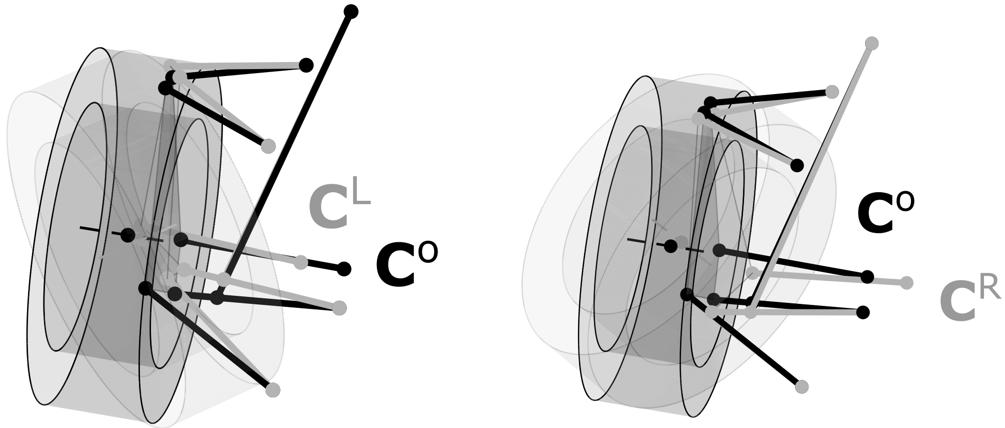

(a) **(b)**

Figure 3.3: Maximum steering angle.

hardpoint change from C to C^L. Figure 3.3a shows the δ_L related to hardpoint C. Similarly, figure 3.3b shows the δ_R related to C^R.

The position constraints for suspension system in figure 3.1 are modelled at [24] in section 3.1.1. The method to reverse the Ackermann percentage design is started by considering the input targets. Table 3.5 shows the input parameters for Ackermann percentage control targets. R_s is the maximum rack travel as per side. δ_L is inner turning angle at maximum rack travel. δ_R is outer turning angle at maximum rack travel. The optimized hardpoint is C'. According to [24] and Paper A, hardpoint component C'_z is controlled by the jounce target 1$^{\text{st}}$ Bump Steer, the hardpoint C' and C can be calculated through an optimization program. Combined with section 3.1.1, all hardpoints can be calculated according to tables 3.3, 3.4 and 3.5.

δ_L
δ_R
R_s

Table 3.5: Ackermann angle control targets.

3.2 Suspension compliance design

The compliance design of wheel suspension involves many components. Bushing elasticity is one of the most important compliance factors that significantly influences the driving behavior. The deformations of the bushings change the wheel orientations when forces are applied on the tire contact patch. Another important factor of the bushing compliance is to provide a comfort driving experience by isolating the vibrations from road irregularities. However, the driving comfort and driving dynamics are often in conflict and need to be balanced in terms of bushing compliance design. Specifically, lateral force steer and brake force steer are closely related to safety and stability and compromises must be minimized. The wheel compliance behavior is the combined elasticity effect of all the bushings. The sensitivity analysis helps engineers to understand the critical bushing for certain compliance attributes, but optimal balancing is complicated to understand. The combination of each individual bushing stiffness must be carefully set to achieve an acceptable level of all the attributes. A method to set the bushing specifications automatically according to the compliance targets is proposed by author. The method makes sure the instant motion of wheel meets the targets. The bushing stiffness is calculated according to force distribution and the motion ratio between wheel and each bushing. The method decouples the axial stiffness and radial stiffness. It provides a method to set up the radial stiffness automatically. The new method will reverse the traditional trial-and-error approach, to avoid extensive iterations and significantly reduce the development time.

3.2.1 Linear reverse method

Consider a five link suspension with the bushings only at inner hardpoints, see figure 3.4. The design goal is to set the correct bushing stiffness that allow wheel move in the correct direction. To avoid the kinematic effect due to the spring travel. In this method, the spring is assumed to be rigid, and only the stiffness along the link directions are considered. The method will be dedicated with three parts, targets definition, motion ratio, and force distribution. A linear algebra using superposition method will decouple the bushing effect and solve the stiffness issue.

3.2.2 Compliance targets

The wheel motions under certain force which applied on the tire contact patch are described using compliance targets. The targets describe the motion mainly under braking force and lateral force. Table 3.6 shows the selected targets. The combined compliance effects from all the bushings need to meet the targets in

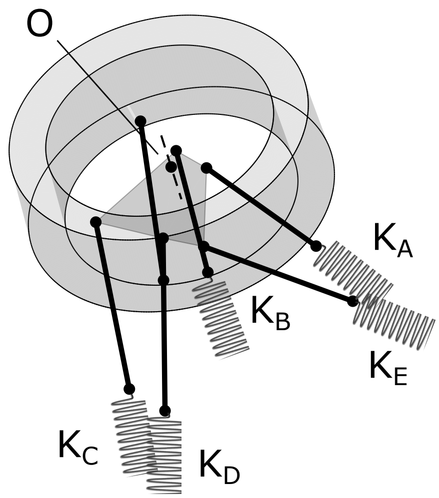

Figure 3.4: Bushing model.

order to provide safe and stable driving behaviors. The targets monitor the toe δ, camber γ, and other motions of wheel center O and contact point P. The definitions are shown in the equations 3.10-3.14.

Brake steer
Longitudinal compliance
Wind-up stiffness
lateral force steer
lateral force camber

Table 3.6: Compliance targets.

$$\text{Brake steer} = \frac{\delta}{F_{px}} \tag{3.10}$$

$$\text{Longitudinal compliacne} = \frac{O_x}{F_{Ox}} \tag{3.11}$$

$$\text{Wind-up stiffness} = \frac{\angle Oy}{F_{px}} \tag{3.12}$$

$$\text{Lateral force steer} = \frac{\delta}{F_{py}} \tag{3.13}$$

$$\text{Lateral force camber} = \frac{\gamma}{F_{py}} \tag{3.14}$$

The targets identified above are the motion gradients from the combined bushing effects. Therefore, the targets should be identified as time derivatives from equations 3.10-3.14. To simplify the expression, static toe and camber angle assume to be zero. Then the targets are modified as following expressions.

$$\frac{d}{dt}\text{Brake steer} = \frac{\omega_z}{F_{px}} \tag{3.15}$$

$$\frac{d}{dt}\text{Longitudinal compliacne} = \frac{V_{Ox}}{F_{Ox}} \tag{3.16}$$

$$\frac{d}{dt}\text{Wind-up stiffness} = \frac{\omega_y}{F_{px}} \tag{3.17}$$

$$\frac{d}{dt}\text{Lateral force steer} = \frac{\omega_z}{F_{py}} \tag{3.18}$$

$$\frac{d}{dt}\text{Lateral force camber} = \frac{\omega_x}{F_{py}} \tag{3.19}$$

Motion ratio calculation

To capture the motion of wheel center O from the movement of the individual bushing, the motion ratios need to be calculated according to kinematic constraints. A model-based linearized constraint was introduced by Matschinsky [1]. This section will modify the method and obtains the motion ratios between the wheel center and bushing radial direction. To model the kinematic constraints, two types of constraints are shown in figure 3.5. They are distinguished by spring link and support link. The motions at wheel $\hat{\mathbf{V}}_O$ and $\hat{\omega}_O$ are interested with the given velocity at hardpoints A, B, C, D, and E. Equation 3.20 shows the motion depend on the hardpoint and input velocity at each inner hardpoint. Assume a constant velocity v is applied on each inner hardpoint, therefore the motions at wheel center O are proportional to v for each specific hardpoint configuration.

$$[\hat{\mathbf{V}}^i_O, \hat{\omega}^i_O] = f_i(\text{HP}, \hat{\mathbf{V}}_i) \tag{3.20}$$

where,

$$i = A, B, C, D, E$$

To calculate the motion at the wheel center O, the velocity constraints for the spring link and the support links need to be constructed. To simplify the

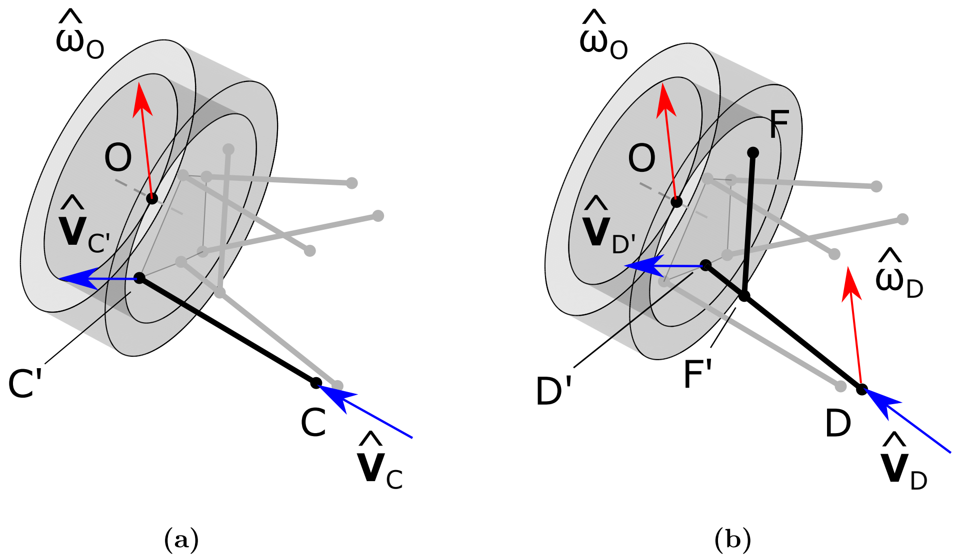

Figure 3.5: Motion ratio calculation.

expression, the unknown parameters are $\hat{\mathbf{V}}_{D'}$, $\hat{\omega}_O$, and $\hat{\omega}_D$.

For spring link,

$$\hat{\mathbf{V}}_{D'} + \hat{\omega}_D \times \mathbf{L}_{D'D} = \hat{\mathbf{V}}_D = v \cdot \hat{\mathbf{e}}_{D'D} \tag{3.21}$$

$$(\hat{\mathbf{V}}_{D'} + \hat{\omega}_D \times \mathbf{L}_{F'D}) \cdot \hat{\mathbf{e}}_{F'F} = 0 \tag{3.22}$$

where,

$$\begin{aligned} &\mathbf{L}_{D'D} = d(D'D),\ d \text{ is the euclidean distance} \\ &\mathbf{L}_{F'D} = d(F'D),\ d \text{ is the euclidean distance} \\ &\mathbf{e}_{D'D} \text{ is unit vector of } \mathbf{L}_{D'D} \\ &\mathbf{e}_{F'F} \text{ is unit vector of } \mathbf{L}_{F'F} \end{aligned}$$

For support links,

$$(\hat{\mathbf{V}}_{D'} + \hat{\omega}_O \times \mathbf{L}_{D'i'}) \cdot \mathbf{L}_{i'i} = \mathbf{L}_{i'i} \cdot \hat{\mathbf{V}}_i \tag{3.23}$$

where,

$$\begin{aligned} &\mathbf{L}_{i'i} = d(i'i),\ d \text{ is the euclidean distance} \\ &i = A, B, C, E \end{aligned}$$

In addition to the constraints from equation 3.21 and equation 3.23. The rotation of link $\mathbf{L}_{D'D}$ needs to be specified, for example, $\hat{\omega}_D \cdot \mathbf{L}_{D'D} = 0$. The equations can be written as matrix format with unknown parameters $\hat{\omega}_O$, $\hat{\omega}_D$, and $\hat{\mathbf{v}}_{D'}$. The velocity at hardpoint D' and the rotational velocity can be calculated using linear algebra. The velocity at wheel center O can be calculated from equation 3.24,

$$\hat{\mathbf{V}}_O = \hat{\mathbf{V}}_{D'} + \hat{\omega}_O \times \mathbf{L}_{OD'} \tag{3.24}$$

For given hardpoints, the motion ratios can be obtained by given input velocity at each inner hardpoints.

$$[\hat{\mathbf{V}}_O^i, \hat{\omega}_O^i] = f(|\hat{\mathbf{V}}_i| = v, |\hat{\mathbf{V}}_{else}| = 0) \tag{3.25}$$

where,

$$i = A, B, C, D, E$$

$$[\hat{\mathbf{V}}_O^i, \hat{\omega}_O^i] = f_i(v) \tag{3.26}$$

where,

$$i = A, B, C, D, E$$

Force distribution

From equations 3.21, 3.22 and 3.24, it is possible to form a linear matrix to solve the kinematic constraint equations to capture the motion at wheel center O. The input velocities from A, B, C, D and E can be expressed as the bushing deformations along the link directions for a particular load case. The bushing deformations are calculated using Hooke's law equation $F = -K \cdot x$. Where, K is the bushing stiffness and if there is a force F acting on the bushing, it deforms by the amount x in the direction of equilibrium position. Therefore, it becomes necessary to calculate the forces acting on each bush. The wheel suspension system can be divided into individual parts to calculate the force distribution using free body diagram. F_{Px}, F_{Py}, F_{Pz} and M_{Px}, M_{Py}, M_{Pz} be the input forces and moments at the tire contact point in the tire coordinate system. As this paper doesn't focus on the tire, the suspension knuckle and the tire can be considered as a single rigid body.

The force equilibrium equations for the knuckle:

$$F + F_A \cdot \hat{e}_{A'A} + F_B \cdot \hat{e}_{B'B} + F_C \cdot \hat{e}_{C'C} + F_D \cdot \hat{e}_{D'D} + F_E \cdot \hat{e}_{E'E} = 0 \tag{3.27}$$

where,

$$F = \begin{bmatrix} F_{Px} \cdot cos(toe) + F_{Py} \cdot sin(toe) \\ F_{Py} \cdot cos(toe) - F_{Px} \cdot sin(toe) \\ F_{Pz} \end{bmatrix}$$

Taking moment equilibrium about point D':

$$\begin{aligned} (M + (L_{OD'} \times F)) + F_A \cdot (L_{A'D'} \times \hat{e}_{A'A}) + F_B \cdot (L_{B'D'} \times \hat{e}_{B'B}) \\ + F_C \cdot (L_{C'D'} \times \hat{e}_{C'C}) + F_E \cdot (L_{E'D'} \times \hat{e}_{E'E}) = 0 \end{aligned} \tag{3.28}$$

where,

$$M = \begin{bmatrix} Mx \\ My \\ Mz \end{bmatrix} + (L_{P,O} \times F)$$

Notice F and M are the forces and moments at the wheel center in the global coordinate system.

Force equilibrium equations for links can be:

$$-F_i \cdot \hat{e}_{i'i} + K_i \cdot S_i \cdot \hat{e}_{i'i} = 0 \tag{3.29}$$

where,

$$\begin{aligned} K_i &= \text{Bushing radial stiffness at D} \\ S_i &= \text{Bushing deformation at D} \\ i &= \text{A,B,C,E} \end{aligned}$$

Considering the forces are acting along the link direction $i'i$ and the moment equations are eliminated. However, for spring link the moments need to be included due the forces from the spring itself.

Force equilibrium equations for spring link:

$$-F_D \cdot \hat{e}_{D'D} + K_S \cdot S \cdot \hat{e}_{F'F} + K_D \cdot S_D \cdot \hat{e}_{D'D} = 0 \tag{3.30}$$

Taking moment equilibrium about Point D:

$$-F_D \cdot (L_{DD'} \times \hat{e}_{D'D}) + K_S \cdot (L_{DF'} \times \hat{e}_{F'F}) = 0 \tag{3.31}$$

From all these equations, a linear force matrix equation can be formed to calculate the force distribution at different joints and bushings for a particular input load case, and the ratios $\frac{F_i}{F_{Px}}$, $\frac{F_i}{F_{Py}}$, $\frac{F_i}{F_{Pz}}$ for different bushings are calculated. In general, for a given hardpoint setup, the forces in the bushings can be represented as a function of the input force at the tire contact point or at the wheel center.

$$[F_i] = g_i(F_j) \tag{3.32}$$

where,

i = A, B, C, D, E
j = Px, Py, Pz, Ox, Oy, Oz (Input forces at contact point P or at wheel center O)

3.2.3 Target-driven method to set up bushing radial stiffness

From equation 3.27, it is possible to get the motion ratios $\hat{V}_O^i/v_i$ and $\hat{\omega}_O^i/v_i$ for every input at i = A,B,C,D,E. Combining all these equations and allowing bushing deformation to be considered as the input, it is possible to calculate the contribution of each bushing on a particular compliance target. Considering brake steer δ_A as the steer effect caused in the suspension system by the bushing at point A, it can be written as,

$$\delta_A = \frac{\omega_{Oz}}{v_A} \cdot S_A \tag{3.33}$$

The bushing deformation S_A can be written as $S_A = F_A/K_A$

$$\delta_A = \frac{\omega_{Oz}}{v_A} \cdot \frac{F_A}{K_A} \tag{3.34}$$

$$\delta_A = \frac{\omega_{Oz}}{v_A} \cdot \frac{F_{px} \cdot F_A}{F_{px}} \cdot \frac{1}{K_A} \tag{3.35}$$

$$\frac{\delta_A}{F_{px}} = \frac{\omega_{Oz}}{v_A} \cdot \frac{F_A}{F_{px}} \cdot \frac{1}{K_A} \tag{3.36}$$

In the equation above it can be seen that the terms ω_{Oz}/v_A and FA/F_{px} are constant as they are the motion ratio and the corresponding force distribution ratio. The constant terms can be expressed as $\omega_z^{BF}{}_A$ for brake force load case.

$$\frac{\delta_A}{F_{px}} = \frac{\omega_{zA}^{BF}}{K_A} \tag{3.37}$$

Similarly,
Wind-up stiffness:

$$\frac{\angle Oy_i}{F_{px}} = \frac{\omega_{yi}^{BF}}{K_i} \tag{3.38}$$

Lateral force steer:

$$\frac{\delta_i}{F_{py}} = \frac{\omega_{zi}^{LF}}{K_i} \tag{3.39}$$

Lateral force camber:

$$\frac{\gamma_i}{F_{py}} = \frac{\omega_{xi}^{LF}}{v_i} \tag{3.40}$$

where, i = A,B,C,D,E

For longitudinal compliance, the brake force input is considered to be acting directly at the wheel center. So, the term corresponding to moment generated at wheel center due to forces at tyre contact point can be ignored in the force distribution equations for this case.
Longitudinal compliance:

$$\frac{X_i}{F_{Ox}} = \frac{V_{OXi}}{K_i} \tag{3.41}$$

The overall compliance target can be considered as the sum of the individual bushing contribution. So overall brake steer is calculated as,

$$\frac{\delta}{F_{px}} = \frac{\delta_A}{F_{px}} + \frac{\delta_B}{F_{px}} + \frac{\delta_C}{F_{px}} + \frac{\delta_D}{F_{px}} + \frac{\delta_E}{F_{px}} \tag{3.42}$$

$$\frac{\delta}{F_{px}} = \frac{\omega_{ZA}^{BF}}{K_A} + \frac{\omega_{ZB}^{BF}}{K_B} + \frac{\omega_{ZC}^{BF}}{K_C} + \frac{\omega_{ZD}^{BF}}{K_D} + \frac{\omega_{ZE}^{BF}}{K_E} \tag{3.43}$$

Considering 5 compliance targets, 5 linear equations can be formed and from the given compliance target inputs, the bushing radial stiffness can be calculated by inverse matrix operation.

$$\begin{bmatrix} \omega_{ZA}^{BF} & \omega_{ZB}^{BF} & \omega_{ZC}^{BF} & \omega_{ZD}^{BF} & \omega_{ZE}^{BF} \\ V_{OX_A} & V_{OX_B} & V_{OX_C} & V_{OX_D} & V_{OX_E} \\ \omega_{YA}^{BF} & \omega_{YB}^{BF} & \omega_{YC}^{BF} & \omega_{YD}^{BF} & \omega_{YE}^{BF} \\ \omega_{ZA}^{LF} & \omega_{ZB}^{LF} & \omega_{ZC}^{LF} & \omega_{ZD}^{LF} & \omega_{ZE}^{LF} \\ \omega_{XA}^{LF} & \omega_{XB}^{LF} & \omega_{XC}^{LF} & \omega_{XD}^{LF} & \omega_{XE}^{LF} \end{bmatrix} \cdot \begin{bmatrix} \frac{1}{K_A} \\ \frac{1}{K_B} \\ \frac{1}{K_C} \\ \frac{1}{K_D} \\ \frac{1}{K_E} \end{bmatrix} = \begin{bmatrix} \text{Brake steer} \\ \text{Longitudinal compliance} \\ \text{Wind up stiffness} \\ \text{Lateral force steer} \\ \text{Lateral force camber} \end{bmatrix} \tag{3.44}$$

3.3 Target-driven kinematics and compliance design

Paper A and section 3.1 describe the reverse kinematic design method for the front and rear suspension. Paper C and section 3.2 describe the reverse compliance design method. A flow combining the kinematic and compliance design methods will be discussed in this section and the method used in Paper B and Paper C will be demonstrated with a case study in this section. Figure 3.6 shows a flow connecting the kinematics and compliance reverse method for the concept development. The input to the program is the kinematic targets, the control points and the compliance targets. The output is the hardpoints and the bushing specifications. Two judgement processes are involved in the automatic process to check the packaging related issues. Although Paper B shows an automatic packaging method, an expert review is still needed to confirm the quality of the results.

3.3.1 Targets and control points data

The kinematic targets that are shown in figure 3.6 are tabled in tables 3.7, 3.8, and 3.9. The control points are tabled in A.1. The kinematics reverse algorithm will create hardpoints with given input from the kinematics targets and the control points. As a result, the generated hardpoints are shown in table A.2. The next step is to calculate the bushing radial stiffness from compliance reverse algorithm. The compliance targets are shown in table 3.10 are given as input. Then, the bushing stiffness can be generated from the compliance reverse method.

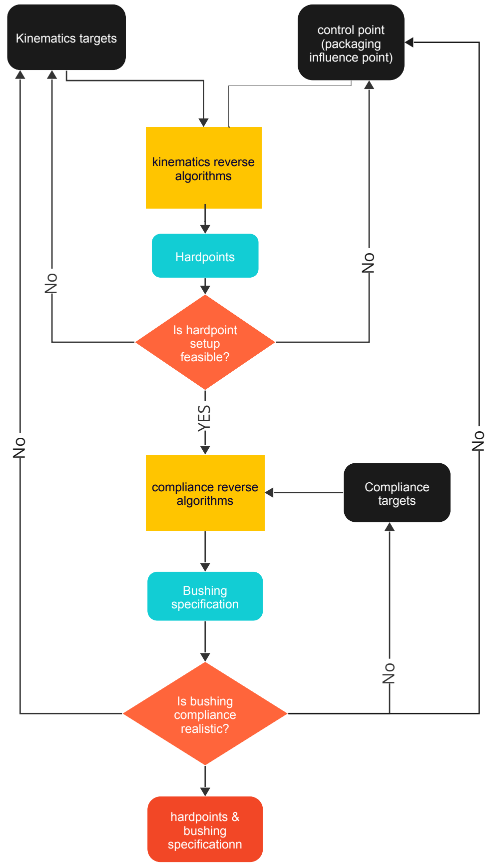

Figure 3.6: Flowchart for concept suspension development.

Target	Value
1^{st} Bump Steer	5.97[deg/m]
1^{st} Bump Camber	-11.94[deg/m]
1^{st} (Kinematic) Anti-lift	0.45[%mm/mm]
1^{st} (Kinematic) Anti-dive	-9.44[%mm/mm]
1^{st} Roll center height (RCH)	67.37[mm]
2^{nd} Bump Steer	-2[(deg/m)/dm]
2^{nd} Bump Camber	-12.17[(deg/m)/dm]
2^{nd} Anti-lift	1.41[%/dm]
2^{nd} Anti-dive	0.73[%/dm]
2^{nd} RCH	-200[mm/dm]

Table 3.7: Jounce targets data.

Target	Value	Target	Value
Hub Trail	1.27[mm]	2^{nd} kingpin angle	-0.094[deg/deg]
Scrub Radius	3.63[mm]	2^{nd} Scrub Radius	2[mm/deg]
Kingpin offset	19.94[mm]	2^{nd} Caster angle	-0.05[deg/deg]
Caster trail	-31.02[mm]	2^{nd}Caster trail	2[mm/deg]
Wheel load lever arm (WLLA)	0.25[mm]	2^{nd} WLLA	0.033[mm/deg]

Table 3.8: steering targets data.

Target	Value
δ_L	-43[deg]
δ_R	35[deg]
R_s	90[mm]

Table 3.9: Ackermann angle targets data.

Target	Value
Brake steer	0.024[deg/kN]
Longitudinal compliance	11048.5[N/mm]
Wind-up stiffness	-0.036[deg/kN]
lateral force steer	-0.032[deg/kN]
lateral force camber	0.015[deg/kN]

Table 3.10: Compliance targets data.

3.3.2 Results

The kinematics simulation results are shown in figure A.1 and the Ackermann behavior are shown in figure 3.8. The simulation result in figure A.1 reflect the targets in tables 3.7 and 3.8. The result matches the targets with small deviation. For example, figure 3.7a from the figure A.1d shows the results of the 1^{st} Bump Steer and the 2^{nd} Bump Steer. The red dashed line shows the slope of bump steer at wheel center. The 2^{nd} Bump Steer is 1.7 [(deg/m)/dm] instead of 2 [(deg/m)/dm] from table 3.7. This is due to the fact that toe δ and camber γ are assumed to be constant when the second order expressions are derived. The simplification causes the deviation of the 2^{nd} Bump Steer. The changes of toe δ and camber γ can be considered to improve the match between the input target and simulation result. However, the simplification reduces the complexity for high order expression. The change of toe δ and camber γ can be excluded by assuming constant value for each simulation step. Figure 3.7b shows that the 2^{nd}

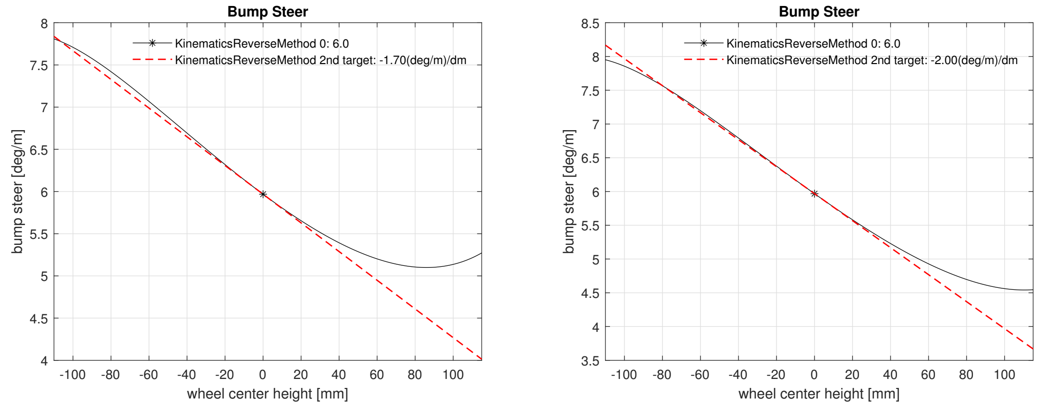

(a) **(b)**

Figure 3.7: Simulation result of bump steer include the effect from toe and camber changes (a), and exclude the effect from toe and camber changes (b).

Bump Steer matches the input targets from table 3.7 when simulation excludes the effect from toe and camber changes. This proves that the reverse algorithm works properly.

The Ackermann behavior also matches the targets in table 3.9. Figure 3.8a shows that the steering angle is 43 deg. for left turn and 35 deg. for right turn with 90 mm rack travel. The simulated results are well-matched with the input targets, which proves that the algorithm works well. Figure 3.8b shows the Ackermann percentage which is calculated using equations 3.6-3.9.

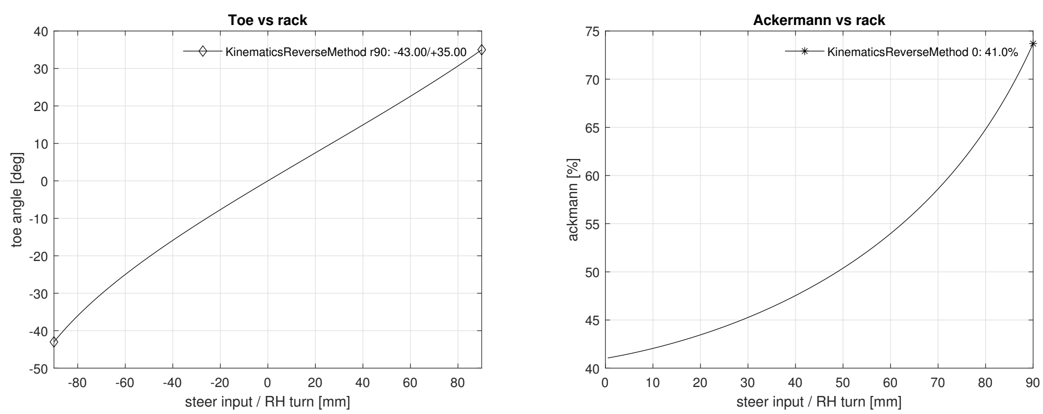

(a) **(b)**

Figure 3.8: Simulation results.

The bushing stiffness that is shown in table 3.11 is the results from the compliance reverse algorithm. Figure 3.11 summarizes the simulation results in figure A.2 and the bushing stiffness from the compliance reverse method. The simulation results that use the bushing stiffness from reverse method give the same value as input target in figure 3.10. Figures A.2b, A.2d, A.2f, A.2h, A.2j show the behaviors of the compliance. The value at wheel center position very well matches the input targets. Therefore, it can be approved the compliance algorithm reverse the compliance design problem successfully. The results from kinematics, Ackermann percentage and compliance behaviors prove that the flow shown in figure 3.6 works well. The hardpoints given in table A.2 and visualized in figure 3.1 fit the design requirements. Furthermore, the compliance behaviors with generated hardpoints have been well controlled by compliance reverse method. The radial stiffness along the link direction has been automatically calculated by the method. The results prove the reverse method works efficiently.

Bushing	**Value**	**Simulation result**	**Value**
A	30000[N/mm]	Brake steer	0.024[deg/kN]
B	6000[N/mm]	lateral force steer	-0.032[deg/kN]
C	60000[N/mm]	lateral force camber	0.015[deg/kN]
D	16000[N/mm]	Wind-up stiffness	-0.036[deg/kN]
E	32000[N/mm]	Longitudinal compliance	11048.5[N/mm]

Table 3.11: Bushing stiffness and simulation result.

Chapter 4

Discussion

The thesis has discussed the important kinematic design method and compliance design method, and Paper B also shows how they are interacting with the packaging method. The discussion in Chapter 4 will bring some important topics related to the reverse design methods. The limitation of the particular methods is also discussed in this chapter. Some intuitive thinking about the future development and improvements will be used to support the argumentation.

4.1 Hierarchical development process

Figure 1.2 shows a traditional V development process. It requires huge mount of iterations between different levels. With the work of target-driven reverse design method, it is possible to automatize one part of the traditional V process. Figure 4.1 highlights a partly automatized process between subsystem level and component level. The components are built automatically according to the component targets, and the subsystem is built consider the best configuration of the components. Therefore, it will be possible to simplify the V process into a hierarchical process which is shown in figure 4.2. As figure 4.2 indicates a much cleaner process to reduce the iterations between subsystem level and component level.

To fully automatize the complete development process is extremely difficult. The method in this thesis only works on kinematics and compliance parts. Some other important attributes such as styling, NVH, durability, structural compliance are not included. All the attributes need to be carefully considered achieving an excellent design. Although the concept development has the limited scope, the work beside the kinematics and compliance is also playing an important role. Beyond the difficult of other important attributes, the goal is replacing the manual iterations by using automatic algorithms. From this perspective, it is still valuable to develop the automatic design algorithms to reduce the development lead time.

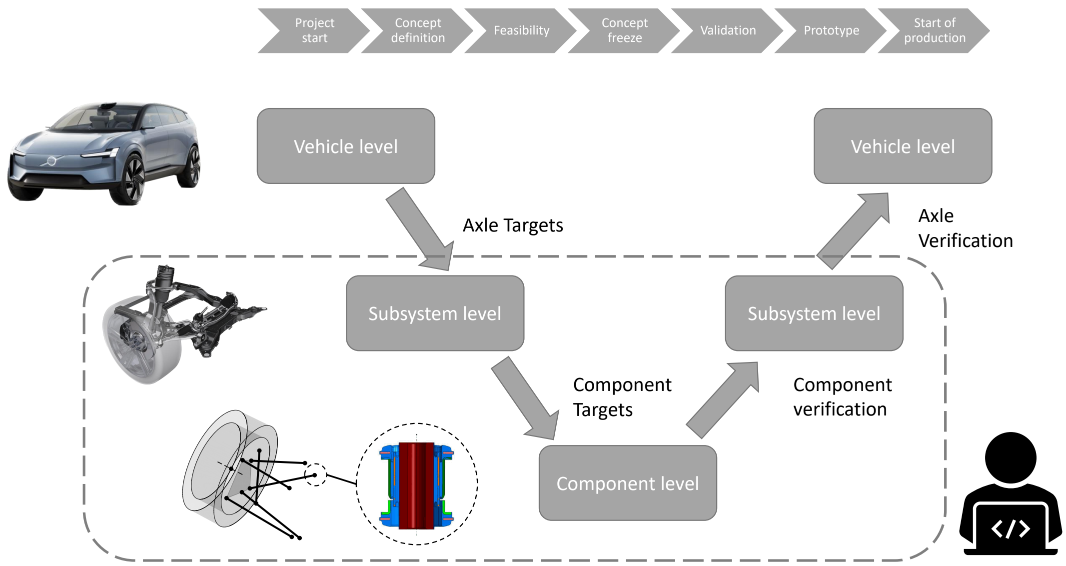

Figure 4.1: Automatized V development process.

4.2 Flexible targets selection

The fundamental idea of the target-driven method is to ensure the design satisfies the targets. However, both kinematics and compliance reverse methods give a fixed scope of selected targets. This is not realistic for real engineering problem. In the suspension development, carry over parts and common parts within platform are common. It means that the component design cannot always be optimized to the performance. Instead, complexity and cost sometime play a critical role. Therefore, a flexible target selection method is needed to balance the overall attributes.

The program mentioned in Paper A given a full scope of targets that can individually be controlled to influence the performance in the best way. However, with pre-fixed hardpoint, some targets are correlated to other targets. It means the targets must be re-balanced. The program also needs to be modified for such purpose. However, it will be difficult to take all the conditions into a universal program. One way to solve it is to provide a flexible program with subroutine that the customer can customize the program.

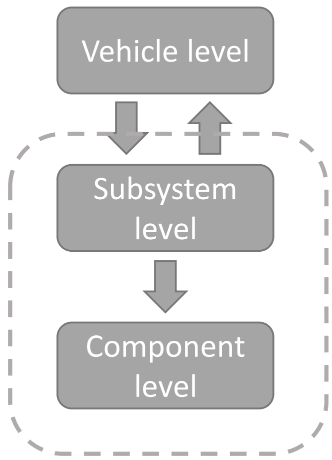

Figure 4.2: Hierarchical process.

4.3 Connect to complete vehicle

The interaction between the complete vehicle and its subsystems are not considered for this thesis. However, the thesis focuses on better component design and subsystem design which is used to improve the behaviors of complete vehicle. So, an efficient flow that connects the subsystem to complete vehicle is also important. There exist the targets cascading method such as [13]. The interest would be to integrate the target-driven reverse method with the targets cascading method in higher level.

4.4 Explore machine learning method

Another interesting factor is exploring how the machine learning method can be used to further reduce the remaining manual work. As artificial intelligence (AI) technology is rapidly growing with more complex nonlinear engineering problems that can be solved by such computational method [25, 26]. AI has evolved in different domains, from playing Atari games, to continuous control reaching superhuman intelligence. Combining machine learning into suspension design area is quite new. For example, reinforcement learning has potential to deploy into suspension development process [27]. It provides the evidences that the machine learning methods has potential to increasing the competence to effectively develop new vehicle concept.

4.5 Application

The reverse method significantly improve efficiency of the kinematics and the compliance design. Thus, it is possible to test a new concept with the support of reverse design method.

Paper B shows a new invented suspension system with carry over targets from combustion engine vehicle to maximize the battery space for electric vehicle [figure 4.3]. This paper demonstrates three showcase studies to solve the packaging issues. During the transformation from a suspension from internal combustion engine (ICE) vehicle to a battery electric vehicle (BEV) adapted suspension, the hardpoints are tuned in such a way that the kinematic behaviors are remaining as much as possible, and the subframe is being moved backward in order to create space for battery. To balance the overall kinematic performance, certain compromises are done for case study 2 and 3. With the traditional trial-and-error method, the tuning process is extremely time-consuming because the tuning loops for kinematics and packaging have to be considered simultaneously. With the automatic tuning method, the kinematics and packaging work are done automatically. Then engineers only need to synchronize the optimization results and adjust the optimization setups if some conflicts are detected. This new method improves the working efficiency dramatically thanks to the automatic tuning algorithms.

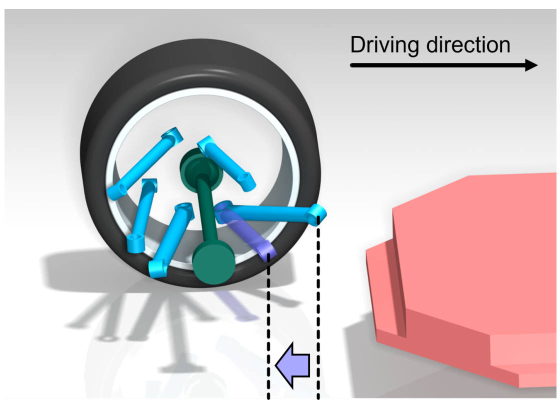

Figure 4.3: Application:Optimized Rear-Axle Concept for Battery Electric Vehicle.

Another application using the reverse design method to lower the engine hood with new invented front suspension [figure 4.4]. With rising customer expectations and additional requirements stemming from the electrification, today's suspensions need to fulfill an increasing number of requirements such as aerodynamic efficiency, driving properties are defined more specifically and the use of carry-over-parts is growing. Moreover, the package volume has a huge effect on the exterior design as well. This leads to complications in the pre-development process. A typical problem is the sequence of development steps: if a completely new suspension has to be defined, is it more important to optimize the hard points and adjust the part geometry accordingly or vice versa? The common approach of a trial-and-error method is time-consuming, since the design of a suspension concept takes days of engineering work.

This approach is demonstrated by designing an optimized five link suspensions for battery-electric vehicles. Additionally, the shape of the suspension volume should be modified in a way, that the height of engine hood can be lowered. Therefore, the aerodynamic behavior has potential to be improved. Furthermore, the new design language for electric car can be achieved with a lowered engine hood. It is found that a feasible solution is possible.

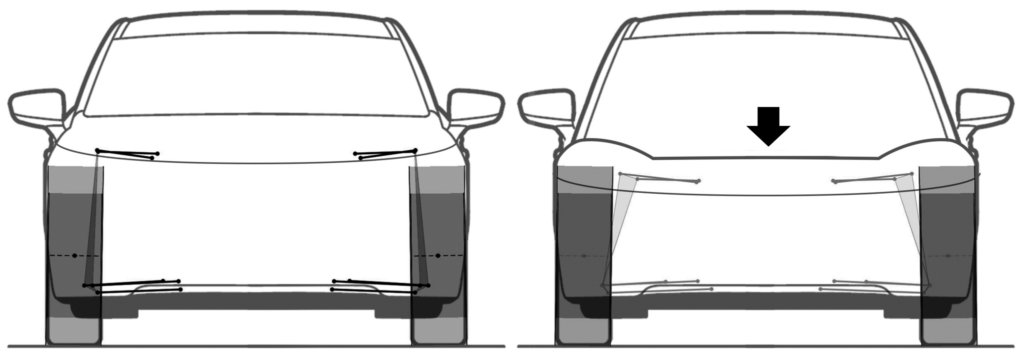

Figure 4.4: Application:Automated Methods for the suspension pre-development.

Chapter 5

Summary

5.1 Conclusion

The target-driven suspension design method reverses the traditional simulation based trial-and-error method. The goal is to reduce the design lead time, thus a later change in a project is possible. Furthermore, an innovative suspension concept can be developed much easier with the reverse design method. The target-driven method also creates a bridge between subsystem design and component design. It means once the targets are set by attribute leader, the method will automatically bring the design into component level. This allows the design engineers focus on other important design factors other than waiting for simulation. The reverse design algorithm also provides an interface that packaging engineer and vehicle dynamic engineer can communicate more efficiently. The results at section 3.3.2 prove the methods from section 3.1 and section 3.2 work efficiently. For a suspension concept development, section 3.3 proposes a flow that combined both kinematics and compliance methods. With the discussion from chapter 4, the method even connects to the complete vehicle level in a structured way. A flexible algorithm will meet the requirements from variable concept design tasks. Some innovation ideas using the reverse method are shown and proposed in section 4.5. The target-driven suspension design method significantly change the way of working in wheel suspension development. It makes the team working in a more agile way. The proposed method reduces the design lead time significantly, thus the development can quickly be adapted to the challenge from market changes especially for electric vehicles. As a result, an agile way of working is truly boosted by the target-driven suspension design method.

5.2 Future work

Future work should focus on further improving the reverse design method and adapting the method to more different design scenarios. The research to investigate the influence of kinematics and compliance behaviors from control point is interesting. How can the structural compliance contribute to the overall wheel suspension behavior? A template model of the structural behavior and adaption of the design with structure compliance targets is also of great interest. The reverse compliance method controls the nonlinear compliance behaviors with axial and radical stiffness is another important topic. The nonlinear bushing model should be able to use in the reverse algorithms as well. The connection to the complete vehicle is also important, using state-of-the-art methods such as reinforcement learning to automatically set the best suspension tuning parameters to fulfill the complete vehicle attributes.

Appendix A

Appendix

A.1 Hardpoint data

Table A.1: Control point

Control point	data	Control point	data
O_x	0	D_x^o	-39
O_y	-817	D_y^o	-348
O_z	191.6	D_z^o	55
A_x^o	-105	E_x^o	331
A_y^o	-456	E_y^o	-392
A_z^o	607	E_z^o	92
B_x^o	177	F_y'	-636
B_y^o	-443	F_z	863
B_z^o	582	-	-
C_x^o	-117	-	-
C_y^o	-355	-	-
C_z^o	89	-	-

The unit of hardpoint use millimeter [mm]

Table A.2: Hardpoint list

Control point	data	Control point	data
O_x	0	-	-
O_y	-817	-	-
O_z	191.6	-	-
A_x	-94.5	A'_x	15.87
A_y	-479	A'_y	-721.1
A_z	607.8	A'_z	616.1
B_x	152.7	B'_x	59.6
B_y	-501.3	B'_y	-725
B_z	590.3	B'_z	621.9
C_x	-120.9	C'_x	156.1
C_y	-393.3	C'_y	-743.3
C_z	87.1	C'_z	69.9
D_x	-36.9	D'_x	-17.2
D_y	-385.1	D'_y	-723.4
D_z	53.6	D'_z	41.1
E_x	-277.8	E'_x	12.3
E_y	-456.4	E'_y	-777.54
E_z	-88.3	E'_z	69.71
F_x	60.2	F'_x	-22.3
F_y	-367.6	F'_y	-636
F_z	863	F'_z	44.4

The unit of hardpoint use millimeter [mm]

A.2 Simulation results

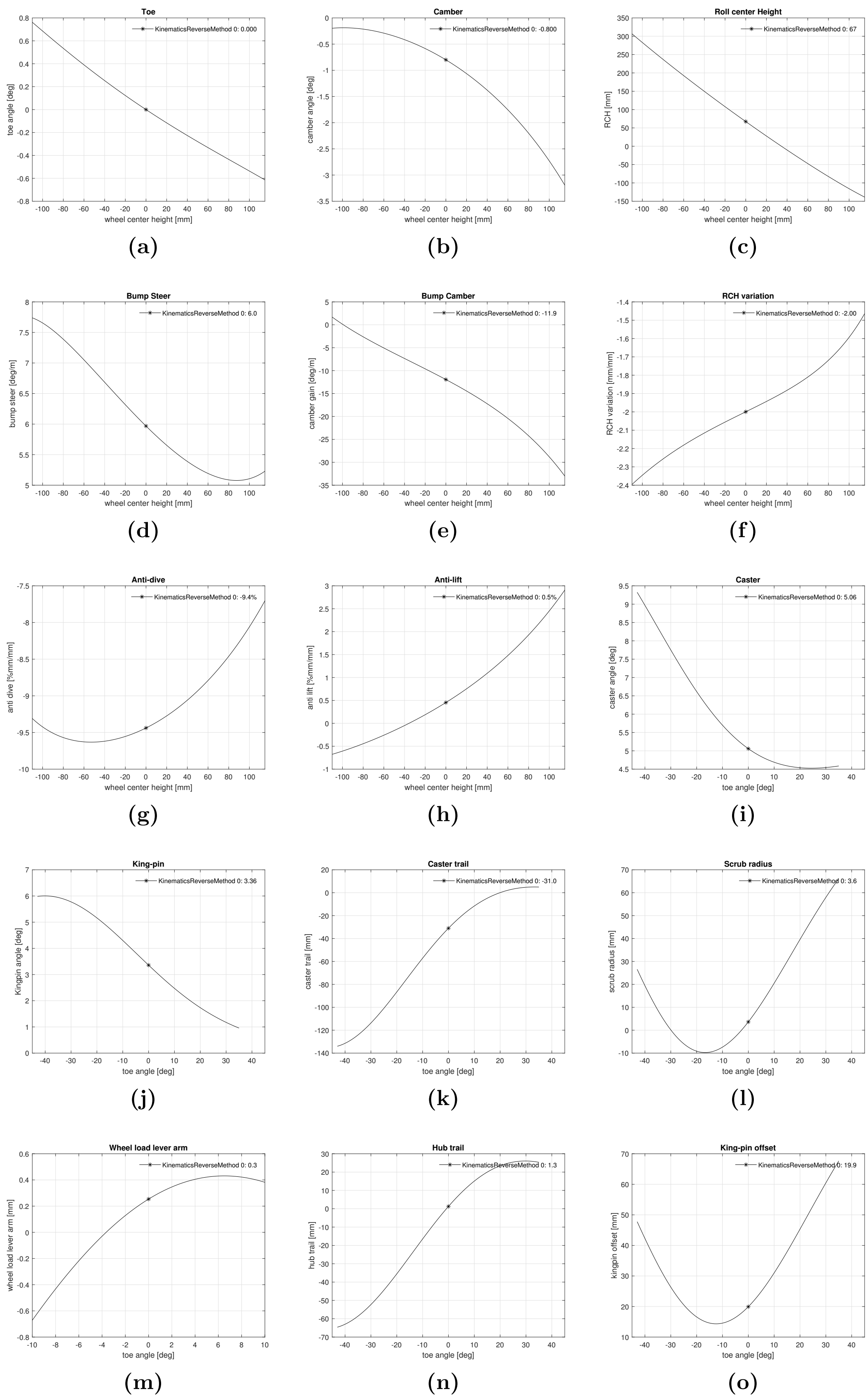

Figure A.1: Result from kinematics simulation.

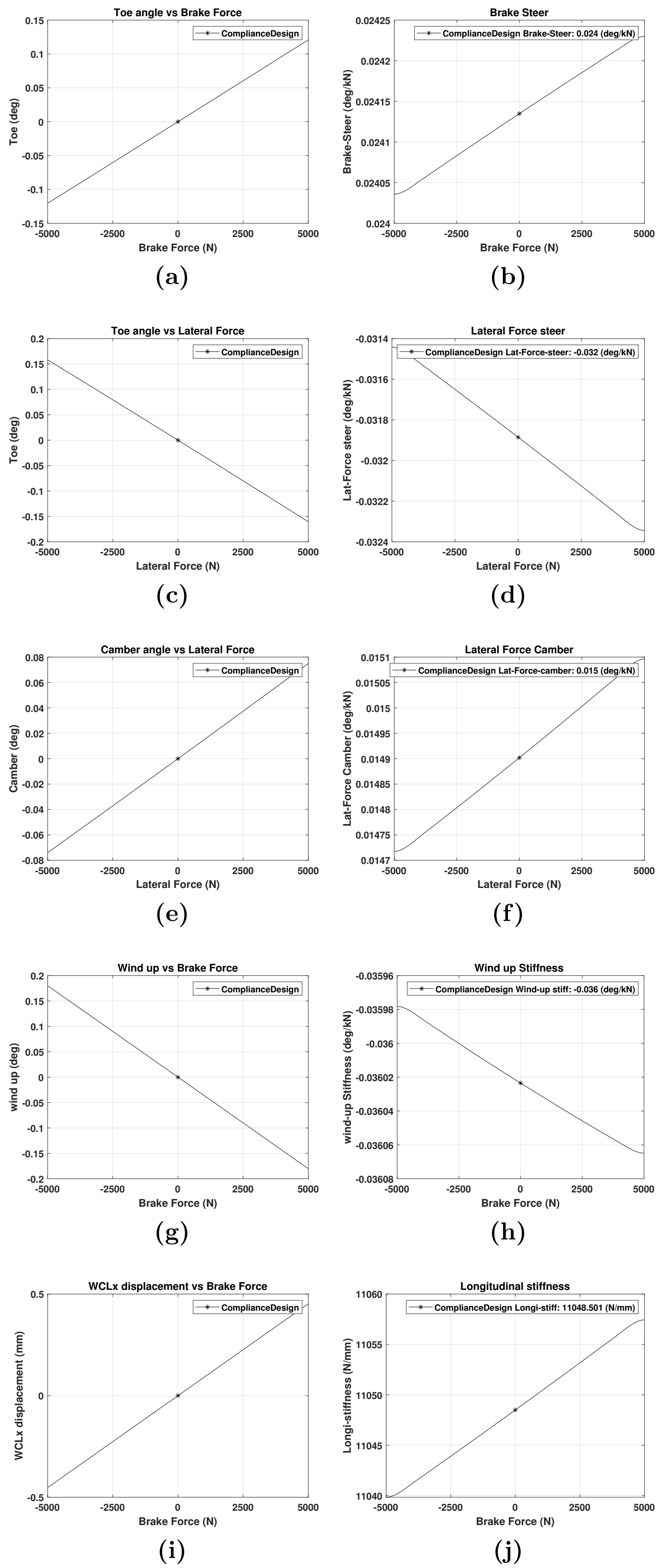

Figure A.2: Result from compliance simulation.

Bibliography

[1] Mstschinsky, W.: Radführungen der Straßenfahrzeuge: Kinematik, Elasto-Kinematik und Konstruktion. Springer, Berlin Heidelberg New York, 3. Auflage, 2007

[2] Albers, I.: Erstellung eines Berechnungstools zur starrki- nematischen Analyse von Einzelradaufhängungen. : Aachen, Rheinisch-Westfälische Technische Hochschule, Dipl.-Arb., 2003

[3] Hazem, A. A.: Numerical Kinematic Analysis of the Standard Macpherson Motor-Vehicle Suspension System : *KSME International Journal*, 17(12), pages 1961–1968, 2003.

[4] J-H Heo, U-K Lee, S-H Lee: Development of a method to compute the kingpin axis using screw axis theory based on suspension-parametermeasuring device data : Journal of Automobile Engineering, Hyundai Motor Company, Gyeonggi-Do, Republic of Korea.

[5] J. K. Lee, J. K. Shim: Validity and limitations of the kinematic roll center concept from the viewpoint of spatial kinematics using screw theory : International Journal of Automotive Technology, 12(5), pages 769–775, 2011.

[6] H. J. Sommer III: Determination of First and Second Order Instant Screw Parameters from Landmark Trajectories : Journal of Mechanical Design, The Pennsylvania State University, University Park, PA 16802.

[7] Volvo Car Corporation: overview chassis concept, internal resource, 2022.

[8] Balakrishna Bhat. A, Naik. A: Master thesis: Suspension Steady-State Kinematics and Compliance Analysis Based On Linear Bushing Model : Institut für Verbrennungsmotoren und Kraftfahrwesen, Universität Stuttgart,Chalmers tekniska högskola / Institutionen för mekanik och maritima vetenskaper, 2020.

[9] Kang, J.S., Yun, J.R., Lee, J.M. and Tak, T.O.: Elastokinematic analysis and optimization of suspension compliance characteristics : SAE transactions, 12(5), pages 87-93, 1997.

[10] Knapczyk, J., Dzierz˙ ek, S.: Displacement and force analysis of five-rod suspension with flexible joints. : Journal of Mechanical Design, 117(4): 532-538, 1995.

[11] Volvo Car Corporation: : "Volvo Concept Recharge" https://www.media.volvocars.com

[12] Ersoy, M., Elbers, C., Schick, B.: Fahrwerkentwicklung In Ersoy, M Gies, S eds Fahrwerkhandbuch. : ATZ/MTZ Fachbuch Springer Vieweg, Wiesbaden, 2017.

[13] Abel. H., Clauss. R., Wagner. A., Prokop. G.: Chassis Development In The Early Stage Using Analytical Target Cascading Methods. : 25. Aachener Kolloquium Fahrzeug- und Motorentechnik, 2016.

[14] Abel. H., Clauss. R., Wagner. A., Prokop. G.: Analytical extension of the effective axle characteristics concept for the development of a structured chassis design process. : Vehicle System Dynamics: International Journal of Vehicle Mechanics and Mobility 55, Nr. 9, S. 1297–1320, 2017. http://dx.doi.org/10.1080/00423114.2017.1309055 DOI 10.1080/00423114.2017.1309055

[15] Abel, H. ; Clauss, R. ; Wagner, A. ; Prokop, G.: Development of an Axle Design Process for the Chassis Design within the Early Development Stage. : 17. Internationales Stuttgarter Symposium, 2017. http://dx.doi.org/10.1007/978-3-658-16988-6 DOI 10.1007/978–3–658–16988–6

[16] Joacim, G., Diego, Z.: Master thesis: Steering performance dependence on front suspension design: Department of Applied Mechanics, Chalmers university of technology, 2015.

[17] Hans-Hermann, B., Ulrich, S.: Vieweg Handbuch Kraftfahrzeugtechnik. Springer, Fachmedien Wiesbaden, 7. Auflage, 2013.

[18] Karl-Ludwig, H.: Grundlagen Der Kraftfahrzeugtechnik. 2018 Carl Hanser Verlag GmbH Co. KG, 5. Auflage, Chapter 4.4, 2013.

[19] Dixon, John C.: Suspension geometry and computation. John Wiley & Sons Ltd, ISBN 978-0-470-51021-6, Chapter 5, 2009

[20] Lee, U., Ahn, B.: a Method to analysis ”The Imaginary Kingpin Axis” in Multi-link Type Suspension System. Vehicle Suspension and Steering Systems, SAE International, 1993.

[21] Heo, J-H., Lee, U-K, Lee, S-H.: Development of a method to compute the kingpin axis using screw axis theory based on suspension-parameter-measuring device data. Proceedings of the Institution of Mechanical Engineers, Part D: Journal of Automobile Engineering. 2009. DOI 10.1243/09544070JAUTO1004

[22] A. Rahmani Hanzaki, P.V.M. Rao, S.K. Saha: Kinematic and sensitivity analysis and optimization of planar rack-and-pinion steering linkages. Mechanism and Machine Theory 44 (2009) 42–56.

[23] Ramon, S., Pablo, G., Fernando, V., Alfonso, F., and Ana, D.: Kinematic design of double-wishbone suspension systems using a multiobjective optimisation approach. Vehicle System Dynamics, 48:7, 793-813. DOI 10.1080/00423110903156574

[24] H. Yansong: Master thesis: Knowledge & requirements based wheel suspension template : Institut für Verbrennungsmotoren und Kraftfahrwesen, Universität Stuttgart, 2018.

[25] Staub, Selva, et al.: ”Artificial neural network and agility.”Procedia-Social and Behavioral Science 195 (2015): 1477-1485.K. P. Murphy, Machine learning: a probabilistic perspective.MIT press, 2012.

[26] J. H. Holland.: Adaptation in Natural and Artificial System. s. University of Michigan Press, 1975.

[27] Lin, Y.-C., Nguyen, H.L.T., Yang, J.-F., Chiou, H.-J.: A reinforcement learning backstepping-based control design for a full vehicle active Macpherson suspension system. IET Control Theory Appl. 16, 1417–1430 (2022). https://doi.org/10.1049/cth2.12317